Talanta 82 (2010) 1164–1169

Contents lists available at ScienceDirect

Talanta

journal homepage: www.elsevier.com/locate/talanta

Direct electrochemistry of cytochrome c immobilized on a novel macroporous gold film coated with a self-assembled 11-mercaptoundecanoic acid monolayer

Ying Li[a,b,*], Jing Li[b], Xing-Hua Xia[b], Song-Qin Liu[a,**]

[a] School of Chemistry and Chemical Engineering, Southeast University, Sipailou 2#, Nanjing 211189, PR China
[b] Key Laboratory of Analytical Chemistry for Life Science, School of Chemistry and Chemical Engineering, Nanjing University, Nanjing 210093, PR China

ARTICLE INFO

Article history:
Received 13 April 2010
Received in revised form 11 June 2010
Accepted 24 June 2010
Available online 3 July 2010

Keywords:
Direct electrochemistry
Cytochrome c
Macroporous gold
Hydrogen bubble template
Galvanic replacement reaction
Self-assembled monolayer

ABSTRACT

We have successfully constructed a novel gold film with open interconnected macroporous walls of nanoparticles by combining the hydrogen bubble dynamic template synthesis with galvanic replacement reaction. After modified by a self-assembled monolayer (SAM) of 11-mercaptoundecanoic acid (MUA), the three-dimensionally (3D) interconnected macroporous Au film has been used as a biocompatible substrate for the immobilization of cytochrome c. The morphology, structure and electrochemical features of the modified and unmodified macroporous Au films were characterized by field-emission scanning electron microscopy (FESEM), energy-dispersive X-ray (EDX), cyclic voltammetry (CV) and electrochemical impedance spectroscopy (EIS). The results reveal that the resultant films had a large electroactive surface area for high protein loading, enhanced electron transfer of cytochrome c, retained electrochemical activity, good stability and repeatability. And the excellent electrochemical behaviors could be attributed to the hierarchical structure of the macroporous Au film constructed by nanoparticles.

1. Introduction

Cytochrome c (cyt c), a heme-containing redox protein, plays the special physiological function by transferring electrons between cyt c reductase and cyt c oxidase both embedded in the mitochondrial membrane [1–3]. Due to its electron transfer capability, cyt c has potentially electroanalytical application as the third-generation protein-based electrochemical biosensors to detect some small molecules or relative substrates including hydrogen peroxide (H_2O_2) [2], nitrite salt [3], nitric oxide [4], superoxide radical anion [5], halogen oxyanions, ascorbic acid (AA) and L-cysteine (LC) [6]. Compared with other analytical methods, such as spectrometry [7], fluorescence [8], chemiluminscence [9], electrochemical biosensors are promising tools due to their accurate, real-time measurements and practical applications in food, clinical and environmental analyses [10–14].

As is well known, direct electron transfer of proteins is a key element for their application in third-generation protein-based electrochemical biosensors. However, it is difficult for cyt c to undergo a facile electron transfer process at bare electrodes, such as Pt, Hg, Au, Ag, Ni, glassy carbon and p-type silicon, because cyt c adsorbs strongly on the conventional electrodes [10–16]. This strong adsorption process often results in protein denaturation and inhibited electron transfer between protein and the electrodes due to the insulation of the redox group of the protein from the electrodes by electrochemically inactive polypeptide chain in cyt c molecule [3,17]. A successful approach to increasing the electron transfer rate of cyt c on the metal electrodes is to create biocompatible environments on the electrode surfaces by modifying promoters. The most promising promoters are self-assembled monolayers (SAMs) of bifunctional alkanethiolate molecules [18,19]. This type of alkanethiolate molecules contains thiol functional groups which covalently bind the promoters to the electrode surfaces and carboxylic functional groups which are available to covalently bind to the $-NH_2$ of lysine residues surrounding the partially exposed heme in cyt c molecule. Covalent binding method can easily retain the bioactivity, electrochemical activity and stability of the immobilized proteins compared with physical adsorption or entrapment [2,16,20,21]. 11-Mercaptoundecanoic acid (MUA) is a typical alkanethiol molecule and can form a stable, tightly packed, low dielectric and ordered hydrocarbon monolayer for the immobilization of cyt c on electrode surface via covalently bound [18,22].

With the development of nanotechnology, many nanostructured Au materials [11,13–15] were used as electrodes for promoting electron transfer of the hemeproteins, and consequently for constructing a third-generation biosensor with high sensitiv-

* Corresponding author at: School of Chemistry and Chemical Engineering, Southeast University, Sipailou 2#, Nanjing 211189, PR China. Tel.: +86 25 52090613; fax: +86 25 52090618.
** Corresponding author. Tel.: +86 25 52090613; fax: +86 25 52090618.
E-mail addresses: wwwli.ying@yahoo.com.cn (Y. Li), liusq@seu.edu.cn (S.-Q. Liu).

0039-9140/$ – see front matter © 2010 Elsevier B.V. All rights reserved.
doi:10.1016/j.talanta.2010.06.036

ity and selectivity, because Au nanomaterials have many excellent characters, such as good conductivity, large surface area-to-volume ratio and compatibility with protein. Brown et al. [23] obtained reversible electrochemistry of cyt c at Au colloid-modified SnO_2 electrodes. Murata et al. [24] constructed an electrode by casting citrate-reduced Au nanoparticles onto a polycrystalline Au electrode, and obtained the direct electrochemistry of cyt c. Zhu et al. [25] prepared nanoporous Au film materials on transparent ITO substrates by alternatively assembling Au and Ag nanoparticles followed by dissolving Ag nanoparticles in $HAuCl_4$ solution. And the nanoporous Au film showed a fast electron transfer of cyt c.

It is well known that an increase in protein loading on the electrode surface could promise a significant improvement in sensitivity. However, by covalent immobilization, the coverage of protein on sensor surface is limited to a monolayer. Macroporous materials as electrodes exhibit higher electroactive surfaces which are addressable to protein, thus, higher protein loading can be achieved. Moreover, three-dimensional macroporous materials could also act as scaffolds for the immobilization of biomolecules and functionalization of various functional groups, and also provide macroporous channels favorable to the diffusion of electroactive materials. The pore walls of macroporous materials are composed of nanoparticles which could act as electron relay centers to facilitate electron communication between the hemeprotein and the electrode [15].

In our previously work [26], we have developed an approach to fabricating 3D macroporous Au films by combining the hydrogen bubble dynamic template synthesis [27,28] with galvanic replacement reaction. Because Au has the high equilibrium potential for electrodeposition and the low overpotential for hydrogen evolution, electrodeposition of Au using the dynamic hydrogen bubble template approach will result in evolution of hydrogen with relatively high speed simultaneously on the newly electrodeposited Au surface and the substrate. Therefore, it is impossible to form a stable hydrogen bubble flow as dynamic template to prepare macroporous Au films with ordered macroporous structure. In order to prepare 3D ordered macroporous Au films, we firstly adopted hydrogen dynamic template method to prepare macroporous Cu films, and then converted the Cu films to Au films by a galvanic replacement. In this galvanic replacement process, the 3D macroporous structure can be retained. The resultant 3D Au films showed an enhanced electrocatalytic activity towards the oxidation of glucose [26]. Compared with other template methods, this method possesses several advantages: low cost, facile control of structure, and easy preparation including preparation of the template, metal deposition, and elimination of the template [26,29]. In addition, the macroporous Au films have outstanding properties, such as macroporous structures and large surface areas, which could be ideal hosts for biomolecules immobilization [30,31]. Herein, this type of the macroporous Au films was firstly employed as biocompatible matrix and efficient electron communication centers for hemoproteins. Cyt c was covalently immobilized on a MUA SAM modified macroporous Au film. Electrochemical characterizations show that the macroporous Au film electrode modified with MUA SAM provides a favorable microenvironment for cyt c to maintain its native electrochemical activity and realize the direct electrochemistry.

2. Experimental

2.1. Materials

$KAu(CN)_2$ was obtained from Special Chemical Reagent Company of Soochow University (Soochow, China). MUA, cyt c from horse heart and 1-ethyl-3-(3-dimethylaminopropyl) carbodiimide (EDC) were purchased from Sigma–Aldrich (St. Louis, USA). H_2O_2 (30%, w/v), $CuSO_4$, KCl, H_2SO_4, K_2HPO_4, KH_2PO_4, $K_3[Fe(CN)_6]$, $K_4[Fe(CN)_6]\cdot 3H_2O$ and anhydrous ethanol were received from Shanghai Chemical Reagent Corporation (Shanghai, China). All chemicals used in this investigation were of analytical grade and without further purification. In all the experiments, deionized water (>18 MΩ) from a Milli-Q purification system (Billerica, USA) was used. Phosphate buffer solution (PBS, pH 7.0) was prepared with KH_2PO_4 and K_2HPO_4.

2.2. Electrodeposition of macroporous Cu films using the hydrogen dynamic template

An Au disk electrode (diameter 8 mm, 99.99%) was used as the substrate (cathode) for Cu electrodeposition. Prior to use, the Au electrode was mechanically polished to a mirror-like surface with 1.0, 0.3 and 0.05 μm Al_2O_3 slurry consecutively. After utrasonicated in alcohol and water, the well-polished electrode was electrochemically pretreated by cycling the potential between −0.25 and +1.55 V in 0.5 M H_2SO_4 at a scan rate of 100 mV s^{-1} until a stable voltammogram was obtained. Then the gold electrode was rinsed with water. For fabrication of macroporous Cu films, constant current (as high as −0.2 A) was applied in a stationary solution of 0.5 M H_2SO_4 + 0.05 M $CuSO_4$ (without stirring or N_2 bubbling).

2.3. Conversion of the macroporous Cu films into macroporous Au films

The chemical conversion of the macroporous Cu films into macroporous Au films was achieved using a template-engaged replacement reaction between the macroporous Cu films and an aqueous $KAu(CN)_2$ solution. In a typical replacement reaction, a macroporous Cu film electrode was immersed in a 50 mM $KAu(CN)_2$ aqueous solution for 2 h, resulting in a macroporous Au film. Accompanying the galvanic replacement, a small amount of Cu impurity remained in the porous structures. In order to selectively remove Cu impurity from the macroporous gold film, cyclic potential scan was performed in 0.5 M H_2SO_4 solution until no other peak appeared except the characteristics of the Au in the cyclic voltammograms, which demonstrated a macroporous pure Au film electrode was obtained. Finally, the macroporous Au film was washed by water and dried under a high-purity N_2 atmosphere.

2.4. Modification of the macroporous Au film electrodes

The prepared macroporous Au film electrodes were immersed in 10 mM MUA ethanolic solution for approximately 12 h. Then, the resulting electrodes were thoroughly rinsed with ethanol and water to remove the physically adsorbed MUA molecules. In the process of immobilization of cyt c, EDC was selected as a coupling agent to activate the reaction between the –COOH groups of MUA and the lysine residues around the heme cavity of cyt c by immersing the MUA SAM modified gold film electrodes in 20.0 mM EDC solution for 12 h [32]. Thereafter, the EDC-activated electrodes were washed and subsequently incubated in a 10 mM PBS containing cyt c (2.0 mg mL^{-1}) at 4 °C for 12 h to form a covalent bond via the carboxylic groups in MUA and amines of lysine in cyt c. To remove any loosely bound cyt c from electrode surface, the electrodes were rinsed with 10 mM PBS (pH 7.0). By this procedure, cyt c has been successfully immobilized onto the MUA SAM modified macroporous Au electrodes. The electrodes were stored in 0.01 M PBS at 4 °C when not in use.

2.5. Instruments

Electrochemical experiments were performed on a CHI 660C electrochemical workstation (CH Instruments, USA). All elec-

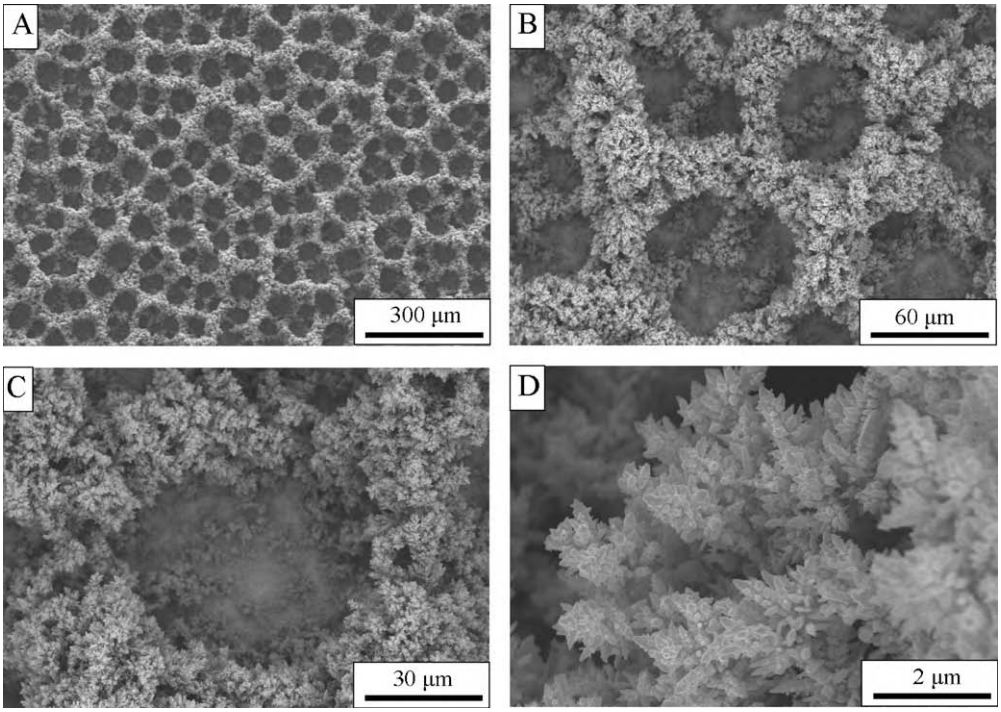

Fig. 1. SEM images (at different magnifications) of the macroporous Cu film electrodeposited using hydrogen bubble as dynamic template at a current of −0.2 A in the electrolyte of 0.05 M $CuSO_4$ + 0.5 M H_2SO_4 for 120 s.

trochemical experiments were carried out with a conventional three-electrode system. A platinum mesh and a saturated calomel electrode (SCE) were used as the auxiliary electrode and the reference, respectively. The modified or unmodified macroporous Au film electrodes were used as the work electrodes. To assess the direct electrochemistry of cyt c, cyclic voltammetry (CV) and electrochemical impedance spectroscopy (EIS) were carried out. EIS was performed in the presence of 5 mM $K_3[Fe(CN)_6]/K_4[Fe(CN)_6]$ (1:1) and 0.1 M KCl with a 5 mV ac amplitude in a frequency range from 0.1 Hz to 100 kHz at the formal potential of $K_3[Fe(CN)_6]/K_4[Fe(CN)_6]$ redox couple. Before electrochemical experiments, the electrolyte was deoxygenated by bubbling highly pure nitrogen for at least 20 min and a nitrogen atmosphere was maintained over the solutions during the measurements. In these experiments, all the potentials referred to the SCE. Field-emission scanning electron microscope (FESEM) (S-5000, Hitach, Japan) equipped with an energy-dispersive X-ray (EDX) system was used to characterize the morphology of the as-prepared electrodes. All electrochemical experiments were carried out at room temperature.

3. Results and discussion

Fig. 1 displays the typical SEM images of the macroporous Cu film electrodeposited at a 0.2 A cathodic current in a 0.05 M $CuSO_4$ and 0.5 M H_2SO_4 solution for 120 s. It is clear that the Cu film is of 3D interconnected macroporous structures and the pore wall consisted of numerous dendrites in all directions. The feature size of the pores in the Cu film is about 70 μm.

The macroporous Cu film has been successfully proved to be an sacrificial template for generating macroporous Au film through a galvanic replacement between the macroporous Cu film and the $KAu(CN)_2$ in solution [26]. In this experiment, the macroporous Cu film was immersed in an aqueous $KAu(CN)_2$ solution, it was then replaced by Au atoms that are deposited epitaxially on the surface of the Cu template, because Cu is more active than Au. Since very stable Au cyanide complex was used, the galvanic replacement reaction occurred very slowly, therefore, the final Au film had essentially the same structure as the porous Cu film. After 2 h galvanic replacement reaction, 93 wt% Cu was converted to Au according to the EDX results [26]. Through an electrochemical clean procedure, the remaining Cu impurity was selectively and gradually dissolved, leaving behind the interconnected macroporous pure Au film. As shown in Fig. 2, the macroporous Au film electrode shows the similar fine structure as the macroporous Cu film, even after the electrochemical purification process for removal of Cu impurity. The as-prepared macroporous Au film shows a hierarchical structure with macropores and nanoparticles. The macropore size is about 30 μm which is restricted compared to the Cu film. The pore wall consists of numerous dendrites in all directions, and its thickness is about 10 μm.

Fig. 3 shows the cyclic voltammograms (CVs) of a smooth Au electrode (a) and a macroporous Au film electrode (b) prepared using the hydrogen dynamic template followed by chemical displacement reaction. The anodic oxidation current starting at about 1.0 V is due to the formation of Au oxide which is subsequently reduced in the negative potential scan, as indicated by the reduction peak at 0.85 V [26]. As shown in Fig. 3, both the porous Au film and the smooth Au electrode show the similar characteristics for a pure Au electrode, suggesting that no Cu impurity remains in the macroporous Au film electrode, in agreement with the EDX data. Electroactive surface area of the macroporous Au film electrode was estimated from the integration of charge required for the reduction of the Au oxide formed in the positive scan in a 0.5 M H_2SO_4, assuming that the reduction of a monolayer of Au oxide requires 386 μC cm^{-2} [26,33]. The electroactive surface areas of the smooth Au and the as-prepared macroporous Au film electrode were calculated to be 2.2 and 43.5 cm^2, respectively, and their corresponding roughness factors (a ratio of the real surface area to the geometric area of 0.5 cm^2) were 4.4 and 87.0, respectively. The roughness factor of the macroporous Au film is higher than those of porous Au films obtained by other methods in the literatures such as template synthesis method [33], dealloying [34], oxidation-reduction [35] and direct hydrogen bubble template method [36].

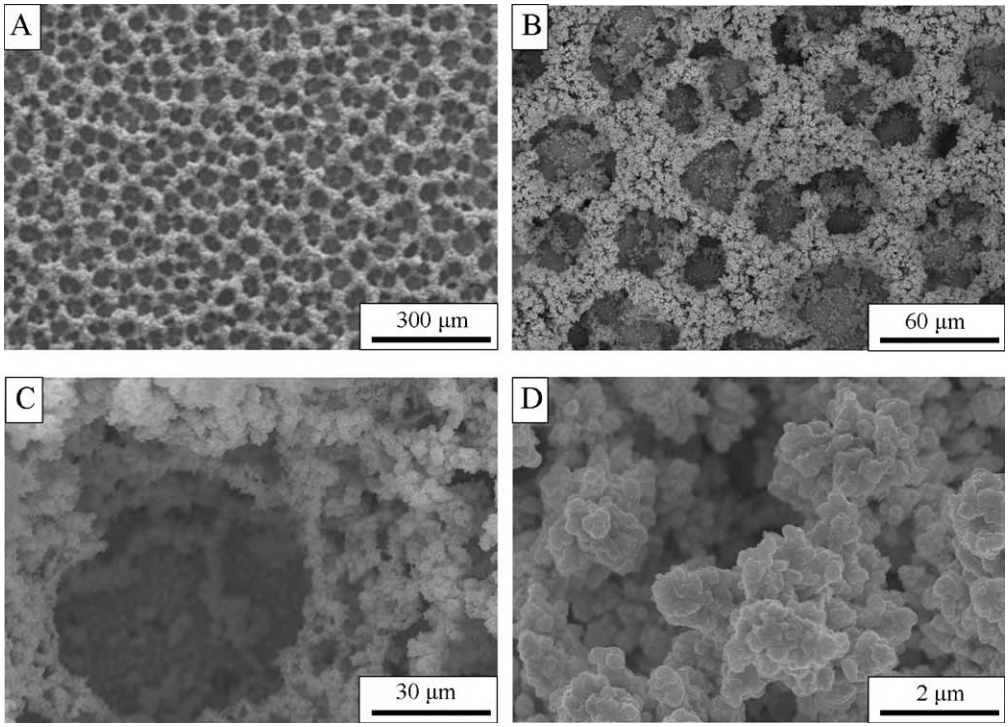

Fig. 2. SEM images (at different magnifications) of the macroporous Au film after galvanic replacement between the porous Cu film and the $KAu(CN)_2$ in solution and electrochemical cleaning process.

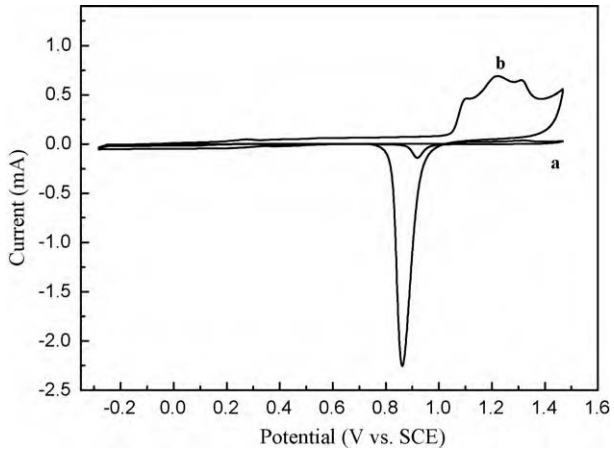

Fig. 3. Cyclic voltammograms (CVs) of a smooth Au electrode (a) and a macroporous Au film electrode (b) in a solution of 0.5 M H_2SO_4 at a scan rate of 10 mV s^{-1}.

Electrochemical impedance spectroscopy (EIS) can provide useful information to characterize interface properties of an electrode surface during the modification process. Using $[Fe(CN)_6]^{3-/4-}$ redox couples as the electrochemical probe, EIS of different layers of the modified electrode was collected. The Randles circuit (insert of Fig. 4A) was chosen to fit the impedance data. It includes the ohmic resistance of the electrolyte solution (R_s), the double-layer interfacial capacitance (C_{dl}) corresponding to the electrochemical charging/discharging process, the electron transfer resistance (R_{et}) corresponding to the electron transfer kinetics of the redox probe at the electrode interface and the diffusion impedance (W) [21,37]. The parallel combination of R_{et} and C_{dl} gives rise to a semicircle. Fig. 4A and B shows the complex-plane impedance spectra (Z'' vs. Z', Nyquist plot) of the EIS obtained at a smooth Au electrode, a porous Au and modified macroporous Au film electrodes. The EIS of the porous Au film electrode (Fig. 4A) shows an almost straight line at all frequencies, which suggests that R_{et} for the electrochemical probe at the macroporous Au film electrode

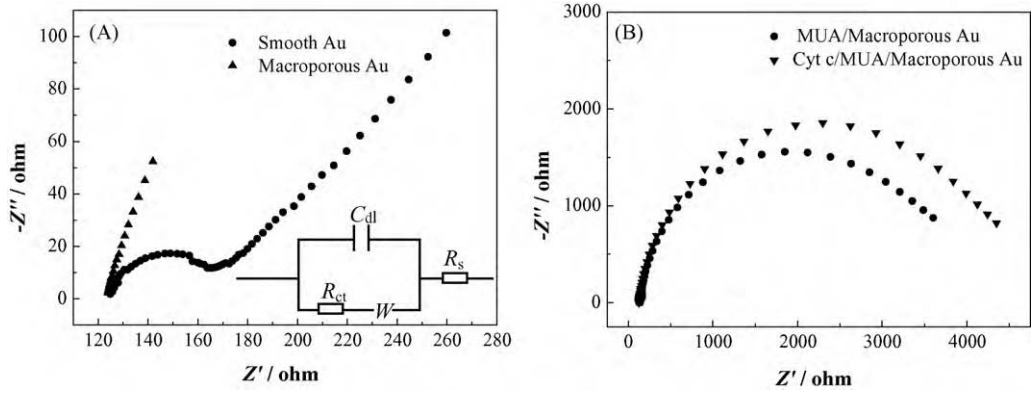

Fig. 4. (A) Nyquist plots obtained at a smooth Au electrode and a macroporous Au film electrode; (B) Nyquist plots obtained at an MUA modified macroporous Au electrode and a cyt c/MUA/macroporous Au electrode. Insert of (A): Randle's equivalent circuit.

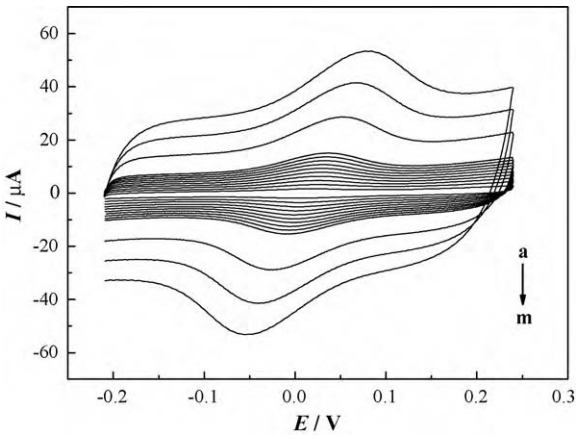

Fig. 5. CVs of cyt c/MUA/macroporous Au at different scan rates in a 0.01 M PBS (pH 7.0). Scan rate from (a) to (m) was 0.01, 0.02, 0.03, 0.04, 0.05, 0.06, 0.07, 0.08, 0.09, 0.1, 0.2, 0.3 and 0.4 V s^{-1}, respectively.

be almost zero. This value is smaller than that of the smooth Au electrode, indicating that electron transfer of the probe is faster at the macroporous Au film electrode than at the smooth Au electrode.

From Fig. 4B, it is apparent that when the macroporous Au film electrode is covered by a monolayer of MUA via Au–S bond, the R_{et} increases dramatically to about 4000 Ω. This phenomenon indicates that the modification of MUA on the electrode surface blocks the electrochemical reaction by an electrostatic repulsion between the negatively charged carboxylic group of MUA and the negatively charged probe ions ($[Fe(CN)_6]^{3-/4-}$) [37]. After the immobilization of cyt c, the R_{et} increases further, demonstrating that cyt c was successfully immobilized on the surface of the MUA modified electrode. The immobilized cyt c further inhibited the electron communication between the electron transfer indicator $[Fe(CN)_6]^{3-/4-}$ and the macroporous Au film electrode surface [38,39]. Cyclic voltammetry was performed to investigate the direct electron transfer of cyt c. Fig. 5 shows the cyclic voltammograms of cyt c immobilized on MUA SAM modified macroporous gold film electrode in a PBS (pH 7.0) at different scan rates. A pair of well-defined and symmetric redox peaks appears, corresponding to the oxidation and reduction of the iron in the heme group. The separation of the redox peak potentials (ΔE_p) is only 3 mV, close to 0 mV, at the scan rate of 10 mV s^{-1}, indicating a fast and reversible surface-controlled electron transfer reaction [40]. The formal potential ($E^{0\prime}$) for the cyt c immobilized on the MUA SAM modified macroporous Au film electrode, being estimated by averaging the redox peak potentials ($E^{0\prime} = (E_{pa} + E_{pc})/2$), is around 0.010 V. This value is in agreement with the formal potential of native cyt c reported as 17 mV in a neutral solution of pH 7.0 [30]. These results clearly demonstrate that MUA SAM plays an important role in the immobilization of cyt c, namely, the proteins chemisorbed on the MUA/macroporous Au film electrode maintain their native electrochemical activity and realizes the direct electrochemistry, which is often very slow at most of the unmodified electrodes [15,16]. MUA is a long-chain thiol which can be chemisorbed on the macroporous Au film surface forming an SAM and give a negatively charged –COOH group for covalent immobilization of cyt c [22]. Such interactions should ensure a largely proper orientation of the immobilization of cyt c and maintain the native properties and reactivity of the protein as it has in its physiological environment [1,15].

As shown in Fig. 6A, both the anodic and the cathodic peak currents increase linearly in the range from 10 to 400 mV s^{-1} with a correlation coefficient of 0.999. These phenomena indicate that the electrode reaction corresponds to a surface-controlled process [20,37,40], verifying that cyt c was stably immobilized on the electrode surface. The redox peak currents (I_p) of the immobilized cyt c on SAM vary with scan rate (υ) following the expression [2,20,21]:

$$I_p = n^2F^2A\Gamma\upsilon(4RT)^{-1} = nFQ\upsilon(4RT)^{-1} \quad (1)$$

where I_p represents the peak current of the anodic or cathodic peak, Q is the quantity of charge calculated from the peak area of the voltammograms, A is the geometric surface area of the macroporous Au film electrode and Γ is the surface coverage of the electroactive substance. The surface coverage (Γ) of cyt c immobilized on the MUA/Au film electrodes can be estimated to be 1.3×10^{-12} mol cm^{-2}, which is in agreement with the theoretical monolayer coverage of 1.4×10^{-12} mol cm^{-2} [21]. Therefore, we can deduce from the results that cyt c is of monolayer modification at the macroporous Au film electrode surface. The number of electron transferred (n) is calculated to be 1.07, close to 1, indicating that all the immobilized cyt c molecules are electroactive and have the favorable orientation [41,42].

As shown in Fig. 6B, with increasing of scan rate, the anodic peaks shift to more positive potentials, while the cathodic peaks shift to more negative potentials. The anodic and cathodic peak potentials are linearly dependent on the logarithm of scan rate (υ) when $n\Delta E_p > 200$ mV, which is in agreement with the Laviron theory [43]. For the cathodic peaks, the slope value is $-2.3RT/\alpha nF$, and for anode peaks, $2.3RT/(1\text{-}\alpha)nF$, where n is the number of electrons transferred in the rate determining reaction, F, R and T have their usual significances. The electron transfer coefficient, α, is estimated to be 0.53. From the peak-to-peak separation in Fig. 6B, the hetero-

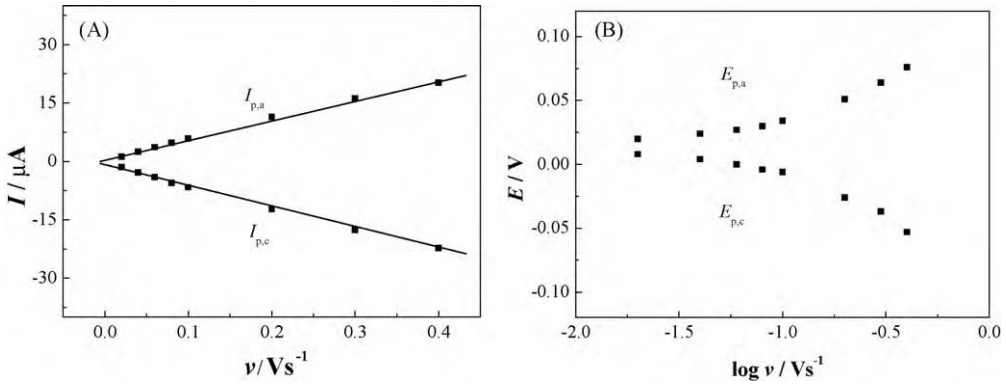

Fig. 6. (A) Plot of the cathodic and anodic peak currents vs. scan rate; (B) Variation of the anodic and cathodic peak potentials vs. the logarithm of scan rate.

geneous electron transfer rate constant (k_s) is determined based on the Laviron's equation.

$$\log\ k_s = \alpha\log(1-\alpha) + (1-\alpha)\log\alpha - \log\left(\frac{RT}{nFv}\right) - \frac{\alpha(1-\alpha)nF\Delta E_p}{2.3RT} \quad (2)$$

where ΔE_p is the peak-to-peak separation. The heterogeneous electron transfer rate constant (k_s) is estimated to be 1.73 s^{-1}. The rate constant k_s is higher than those of cyt c modified electrodes in the literature such as colloidal Au (1.2 s^{-1}) [44], Au nanoparticle (1.06 s^{-1}) [45], Au/Ti (0.142 s^{-1}) [46], Au/TiO_2 (1.04 s^{-1}) [46], Au nanoparticles/chitosan/carbon nanotubes (0.97 s^{-1}) [30], dsDNA/Au (1.4 s^{-1}) [47] and humic acid/Au (1.0 s^{-1}) [48]. The high value of k_s suggests that the MUA SAM modified macroporous Au films act as a good platform for the immobilization of cyt c, and the modified electrode can provide a favorable microenvironment for cyt c to undergo easy and fast electron transfer reaction even at high scan rates.

In addition, it was found that less than 10% of the immobilized proteins desorbed from the cyt c/MUA/macroporous Au film electrode when stored at 4 °C for 15 days. Consecutive potential scan up to 100 cycles of the cyt c-monolayer-modified electrodes in 0.01 M PBS yielded a good repeatable signal with a relative standard deviation of 5.0%, indicating that cyt c was stably immobilized on the macroporous Au film surfaces.

The excellent electrochemical behaviors of the cyt c immobilized on the MUA SAM modified macroporous Au film electrode could be interpreted as follows. First, highly dispersed macroporous Au films provide a larger surface area for the immobilization. Second, the Au nanoparticles on the pore wall may be fit for the orientation of cyt c, and thus make the active center of cyt c closer to the active site of the electrode [46] and facilitate electron transfer between cyt c and the macroporous Au film electrode. In conclusion, the hierarchical structure of the macroporous Au film electrode provides a favorable microenvironment for the immobilization of cyt c and the direct electron transfer between cyt c and electrode.

4. Conclusions

We have successfully fabricated macroporous Au films by combination of hydrogen bubble template with galvanic replacement reaction. On the basis of multiple microstructures and high electroactive surface area, the resulting Au film after modified with MUA is propitious to the covalent immobilization of cyt c and maintains the native bioactivity and electrochemical activity of cyt c. Moreover, MUA SAM modified macroporous Au film electrode can realize the direct electrochemistry of cyt c and ensure the highly stability of the immobilized cyt c. The excellent electrochemical behaviors of the cyt c immobilized on the MUA SAM modified macroporous Au film electrode can be attributed to the hierarchical structure of the macroporous Au film electrodes. This work provides a general method to realize direct electron transfer of electroactive proteins, which promises to develop high performance bioelectronics devices such as biosensors and biofuel cells.

Acknowledgments

This work was supported by the National Natural Science Foundation of China (20828006) and the National Science Fund for Creative Research Groups (20821063).

References

[1] C.L. Xiang, Y.J. Zou, L.X. Sun, F. Xu, Talanta 74 (2007) 206.
[2] Y.N. Zhou, J.F. Zhi, Y.S. Zou, W.J. Zhang, S.T. Lee, Anal. Chem. 80 (2008) 4141.
[3] Q.P. Chen, S.Y. Ai, X.B. Zhu, H.S. Yin, Q. Ma, Y.Y. Qiu, Biosens. Bioelectron. 24 (2009) 2991.
[4] W.C.A. Koh, M.A. Rahman, E.S. Choe, D.K. Lee, Y.B. Shim, Biosens. Bioelectron. 23 (2008) 1374.
[5] S. Shipovskov, E.E. Ferapontova, I. Gazaryan, T. Ruzgas, Bioelectrochemistry 63 (2004) 277.
[6] J.W. Shie, U. Yogeswaran, S.M. Chen, Talanta 74 (2008) 1659.
[7] R. Santucci, E. Laurenti, F. Sinibaldi, R.P. Ferrari, Biochim. Biophys. Acta 1596 (2002) 225.
[8] M.J. Zhou, Z.J. Diwu, N. Panchuk-Voloshina, R.P. Haugland, Anal. Biochem. 253 (1997) 162.
[9] Y. Lv, Z.J. Zhang, F.N. Chen, Analyst 127 (2002) 1176.
[10] M. Zhou, Y.M. Zhai, S.J. Dong, Anal. Chem. 81 (2009) 5603.
[11] E. Katz, I. Willner, J. Wang, Electroanalysis 16 (2004) 19.
[12] P. Kohli, M. Wirtz, C.R. Martin, Electroanalysis 16 (2004) 9.
[13] X.L. Luo, A. Morrin, A.J. Killard, M.R. Smyth, Electroanalysis 18 (2006) 319.
[14] F. Wang, S.S. Hu, Microchim. Acta 165 (2009) 1.
[15] L. Wang, E.K. Wang, Electrochem. Commun. 6 (2004) 49.
[16] H.J. Kim, K.S. Lee, M.S. Won, Y.B. Shim, Langmuir 24 (2008) 1087.
[17] L. Lin, P.H. Qiu, X.N. Cao, L.T. Jin, Electrochim. Acta 53 (2008) 5368.
[18] A.F. Loftus, K.P. Reighard, S.A. Kapourales, M.C. Leopold, J. Am. Chem. Soc. 130 (2008) 1649.
[19] Y.H. Wu, S.S. Hu, Bioelectrochemistry 1 (2006) 105.
[20] D.H. Nagaraju, R.K. Pandey, V. Lakshminarayanan, J. Electroanal. Chem. 627 (2009) 63.
[21] L. Zhang, J. Zhang, C.H. Zhang, Biosens. Bioelectron. 24 (2009) 2085.
[22] J. Grochol, R. Dronov, F. Lisdat, P. Hildebrandt, D.H. Murgida, Langmuir 23 (2007) 11289.
[23] K.R. Brown, A.P. Fox, M.J. Natan, J. Am. Chem. Soc. 118 (1996) 1154.
[24] K. Murata, K. Kajiya, M. Nukaga, Y. Suga, T. Watanabe, N.i. Nakamura, H. Ohno, Electroanalysis 22 (2009) 185.
[25] A.W. Zhu, Y. Tian, H.Q. Liu, Y.P. Luo, Biomaterials 30 (2009) 3183.
[26] Y. Li, Y.Y. Song, C. Yang, X.H. Xia, Electrochem. Commun. 9 (2007) 981.
[27] H.C. Shin, M.L. Liu, Chem. Mater. 16 (2004) 5460.
[28] H.C. Shin, J. Dong, M.L. Liu, Adv. Mater. 15 (2003) 1610.
[29] Y. Li, W.Z. Jia, Y.Y. Song, X.H. Xia, Chem. Mater. 19 (2007) 5758.
[30] L. Zhang, Biosens. Bioelectron. 23 (2008) 1610.
[31] Y.Y. Song, W.Z. Jia, C. Yang, X.H. Xia, Adv. Funct. Mater. 17 (2007) 2377.
[32] E. Katz, I. Willner, J. Am. Chem. Soc. 125 (2003) 6803.
[33] W. Gao, X.H. Xia, J.J. Xu, H.Y. Chen, J. Phys. Chem. C 111 (2007) 12213.
[34] H. Dong, X.D. Cao, J. Phys. Chem. C 113 (2009) 603.
[35] Q.Y. Yang, Y. Liang, T.S. Zhou, G.Y. Shi, L.T. Jin, Electrochem. Commun. 11 (2009) 893.
[36] Y. Chen, X.J. Yang, L.R. Guo, J. Li, X.H. Xia, L.M. Zheng, Anal. Chim. Acta 644 (2009) 83.
[37] Y.J. Yin, P. Wu, Y.F. Lu, P. Du, Y.M. Shi, C.X. Cai, J. Solid State Electr. 11 (2007) 390.
[38] L.Y. Chen, B.X. Gu, G.P. Zhu, Y.F. Wu, S.Q. Liu, C.X. Xu, J. Electroanal. Chem. 617 (2008) 7.
[39] S.Q. Liu, B.P. Lin, X.D. Yang, Q.Q. Zhang, J. Phys. Chem. B 111 (2007) 1182.
[40] C.L. Xiang, Y.J. Zou, L.X. Sun, F. Xu, Electrochem. Commun. 10 (2008) 38.
[41] S. Bernad, T. Soulimane, Z. Mehkalif, S. Lecomte, Biopolymers 81 (2006) 407.
[42] D.H. Murgida, P. Hildebrandt, J. Mol. Struct. 565 (2001) 97.
[43] E. Laviron, J. Electroanal. Chem. 101 (1979) 19.
[44] H.X. Ju, S.Q. Liu, B.X. Ge, F. Lisdat, F.W. Scheller, Electroanalysis 14 (2002) 141.
[45] H.Q. Liu, Y. Tian, Z.F. Deng, Langmuir 23 (2007) 9487.
[46] G.H. Zhao, Y.Z. Lei, Y.G. Zhang, H.X. Li, M.C. Liu, J. Phys. Chem. C 112 (2008) 14786.
[47] H.H. Liu, J.L. Lu, M. Zhang, D.W. Pang, H.D. Abruña, J. Electroanal. Chem. 544 (2003) 93.
[48] J.J. Xu, G. Wang, Q. Zhang, D.M. Zhou, H.Y. Chen, Electrochem. Commun. 6 (2004) 278.